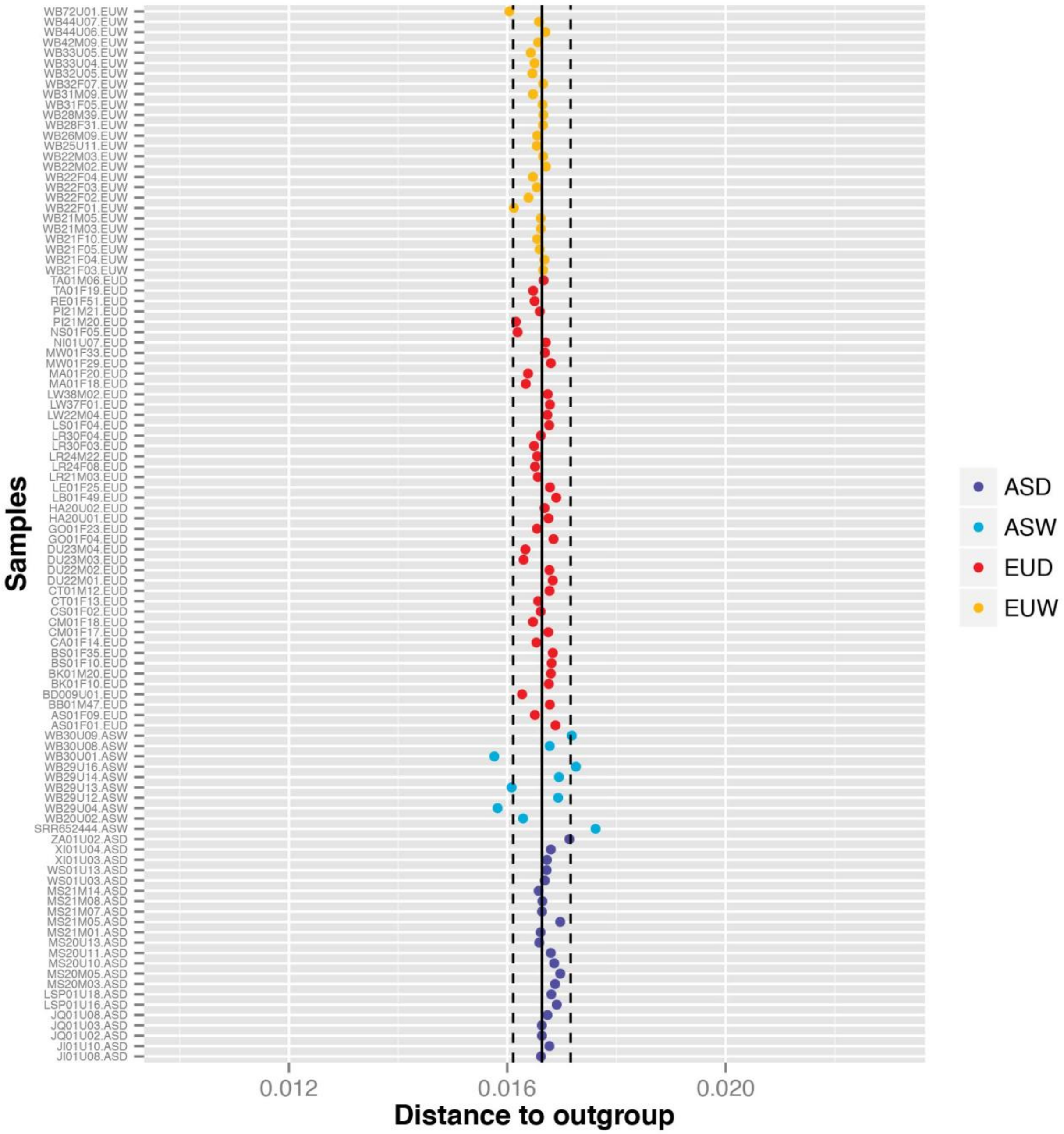

Supplementary Figure 1

Nucleotide distance to the outgroup (*S. verrucosus*).

Each circle represents the mean distance computed in 10-kb windows across the genome. The dashed lines correspond to ±1 s.d. of the mean distance computed across all individuals.

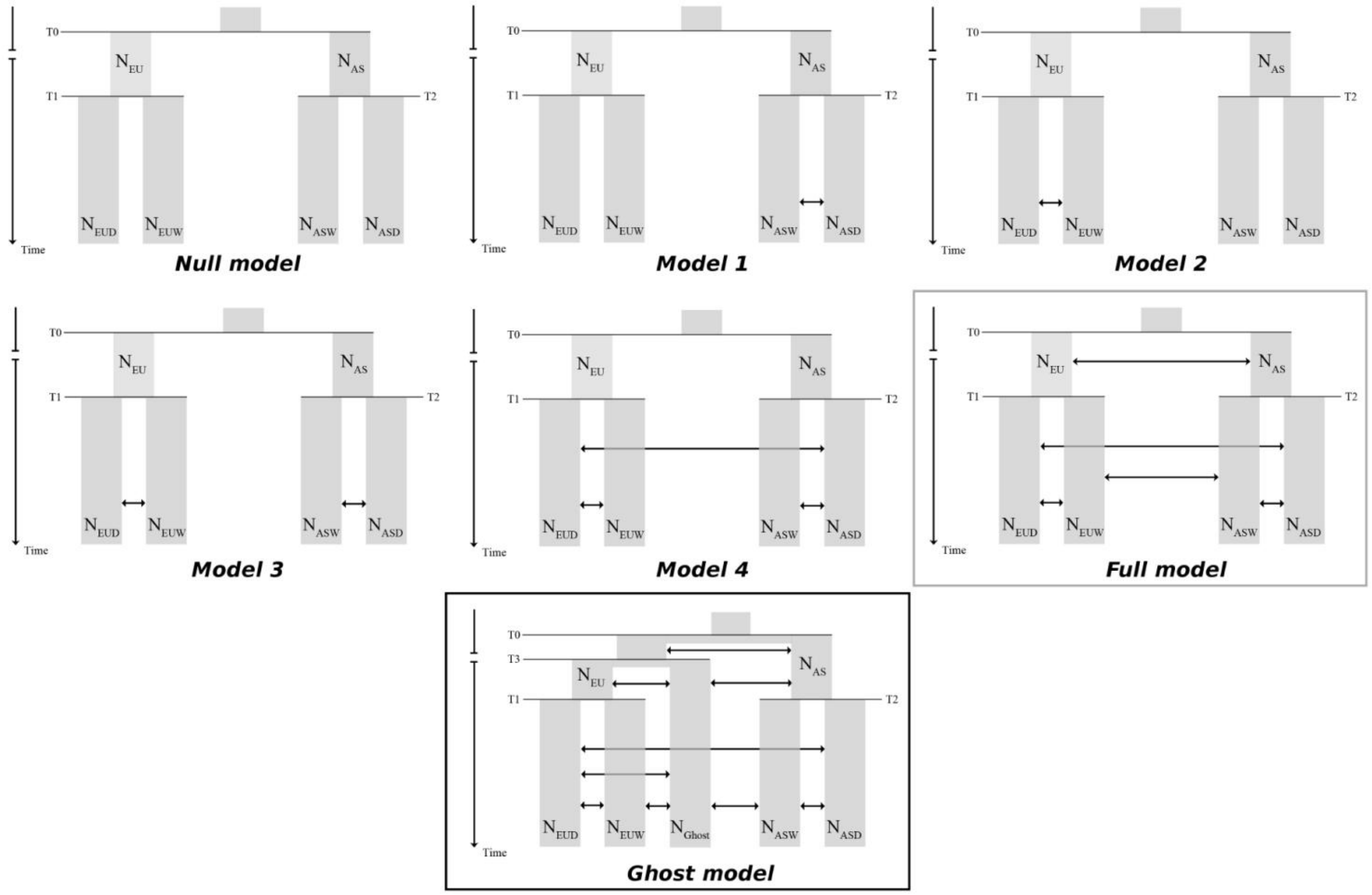

Null model

Model 1

Model 2

Model 3

Model 4

Full model

Ghost model

Supplementary Figure 2

All models investigated in this study.

Schematic of all models tested in this study. The upper six models were first compared together. In this comparison, the full model (outlined with a gray square) was the best-fitting model. When all seven models were tested together, the ghost model had the best fit (outlined with a black square). All priors and support values are reported in **Supplementary Table 5**.

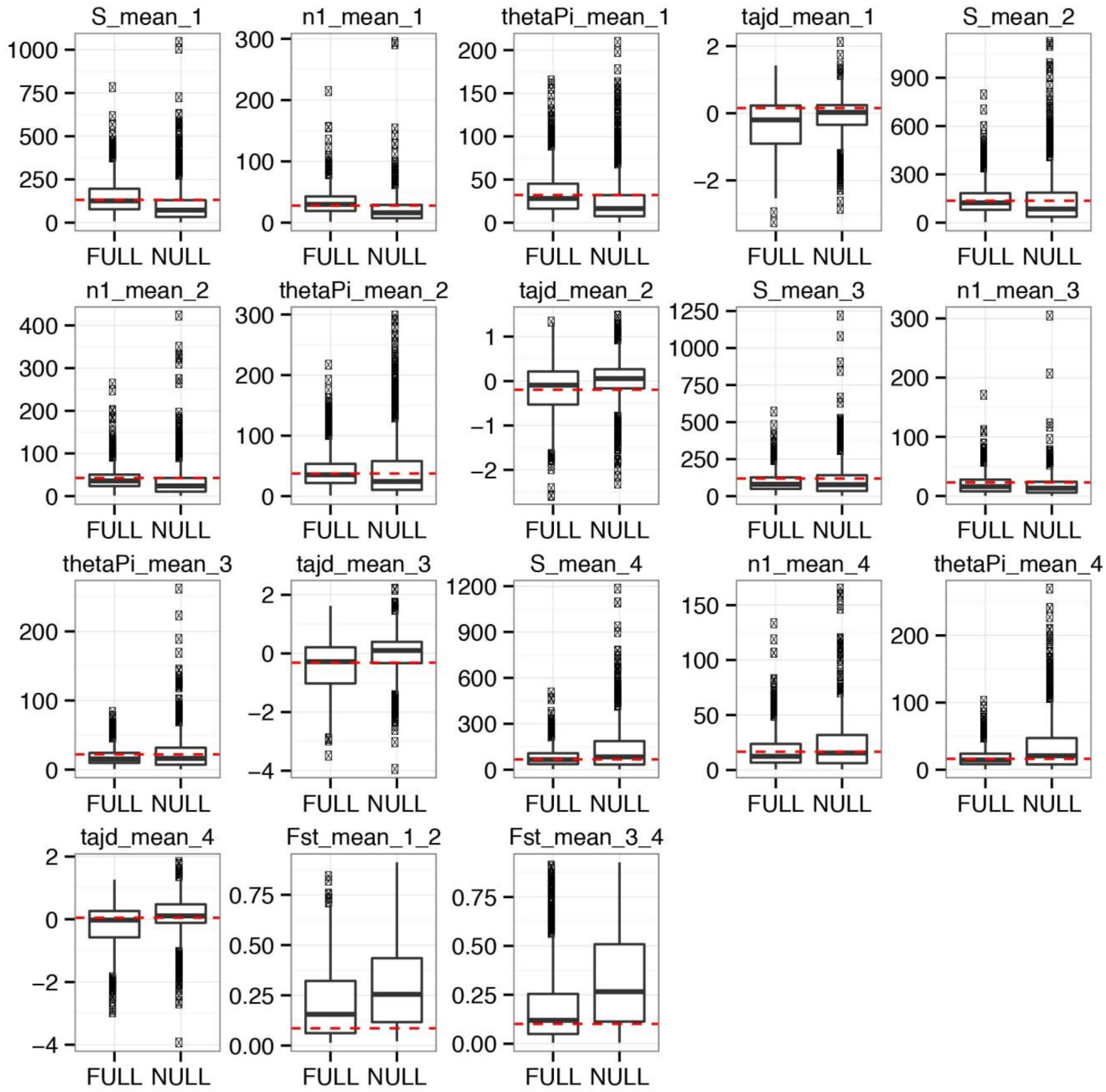

Supplementary Figure 3

Distribution of raw summary statistics under the full and null models.

The dashed red line represents the value of the observed summary statistic. S_mean, mean number of segregating sites; n1, number of singletons; thetaPi, θ_π; tajd, Tajima's *D*.

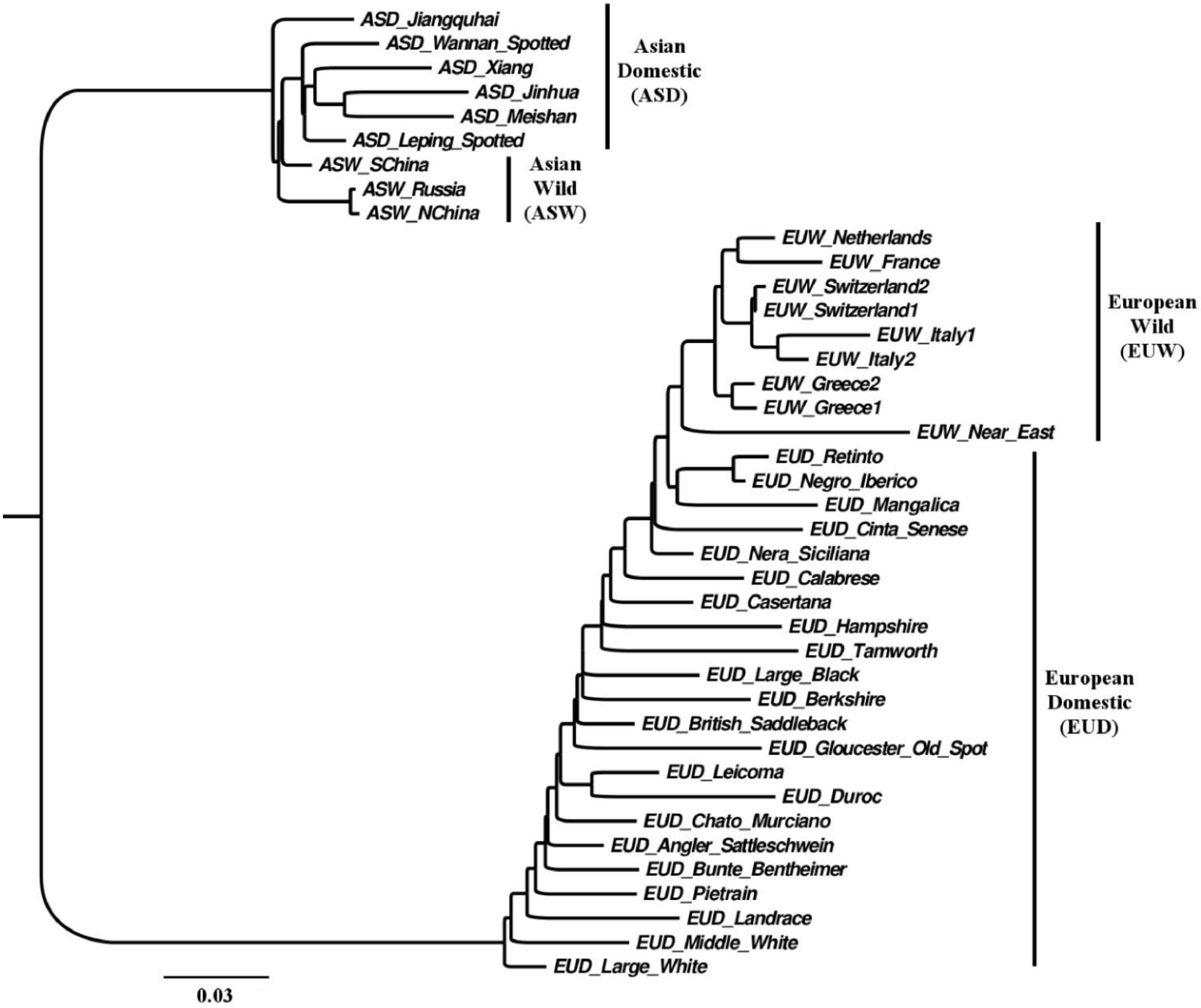

Supplementary Figure 4

Result of the TreeMix analysis for the 602 pigs genotyped on the porcine 60SNP array data set.

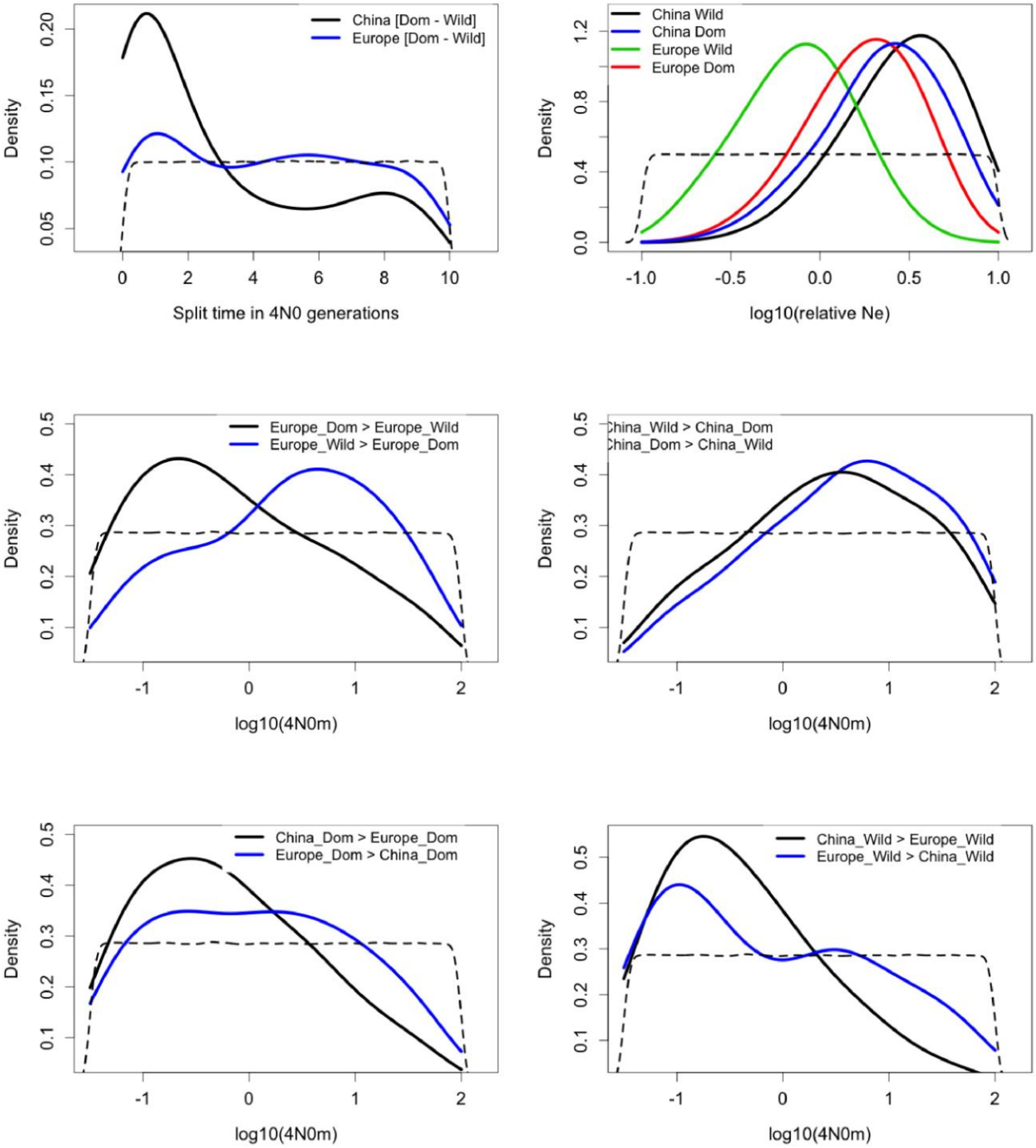

Supplementary Figure 5

Posterior distribution of all parameters in the full model.

Population sizes are the relative population size (the ratio of the current population size over the population size at t_0; **Fig. 1**). Dashed lines represent the prior distributions. The full model is as in **Supplementary Figure 1**.

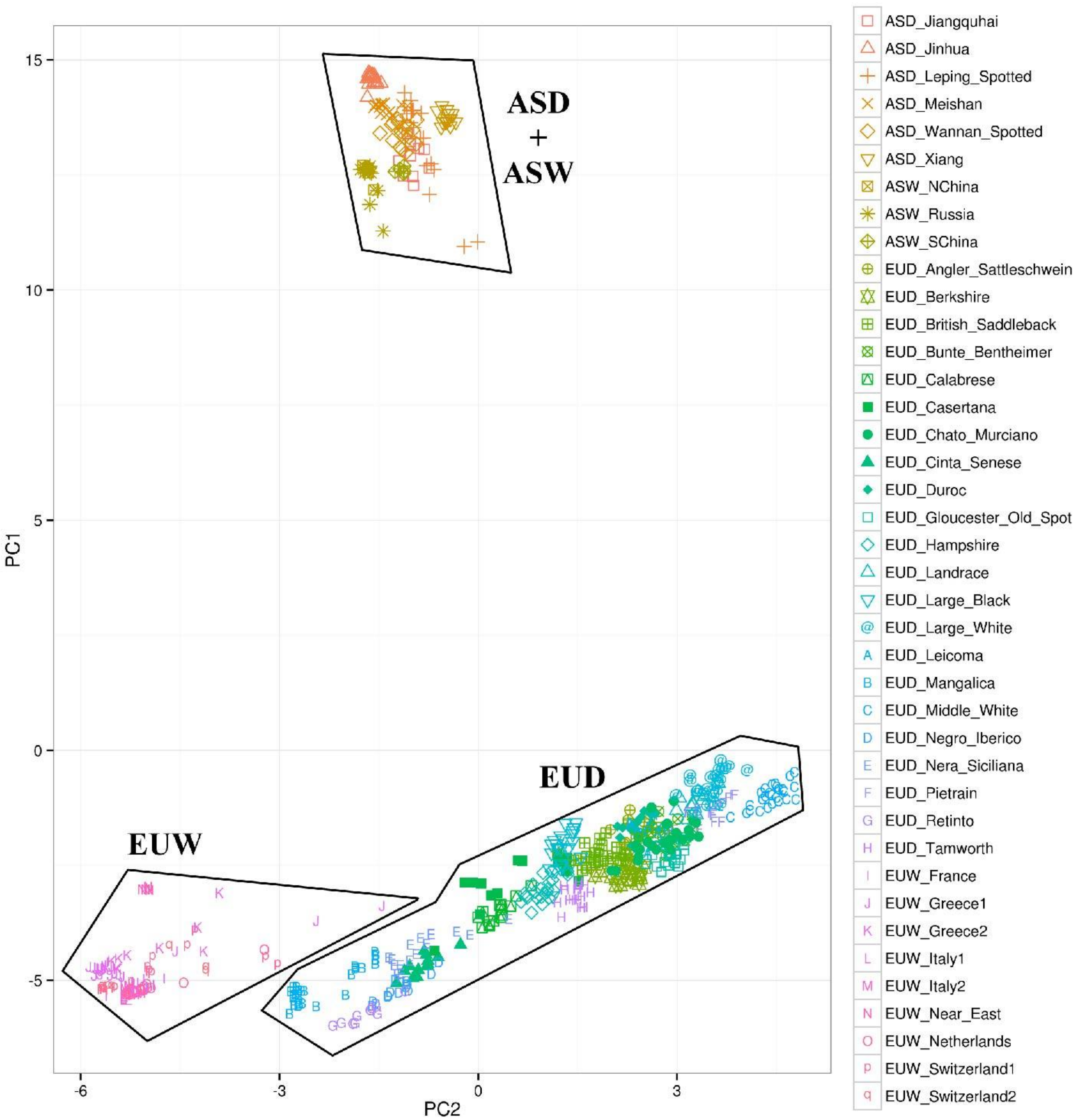

Supplementary Figure 6

Result of PCA (PC1-PC2) based on 602 genotyped pigs.

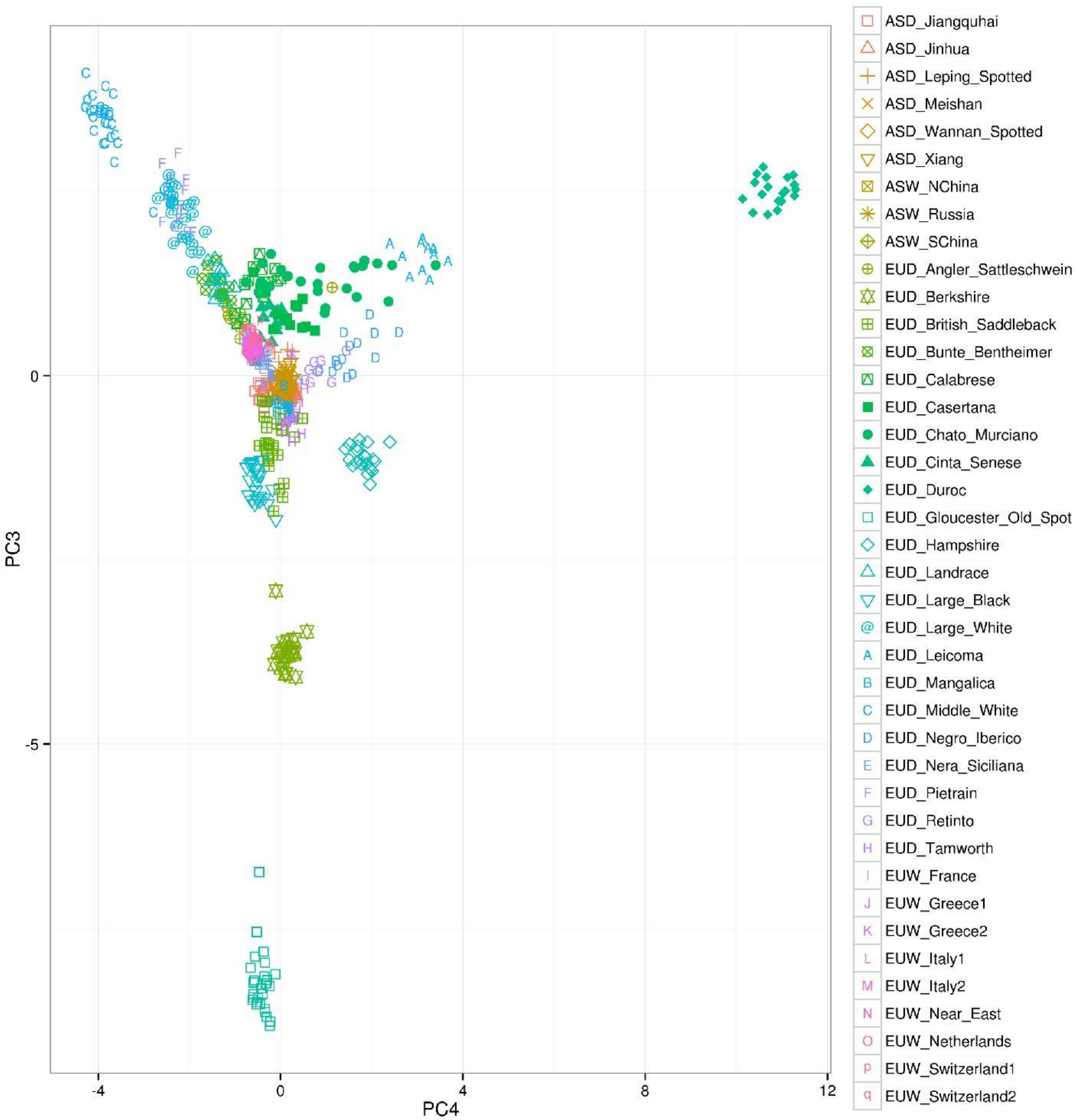

Supplementary Figure 7

Result of PCA (PC3-PC4) based on 602 genotyped pigs.

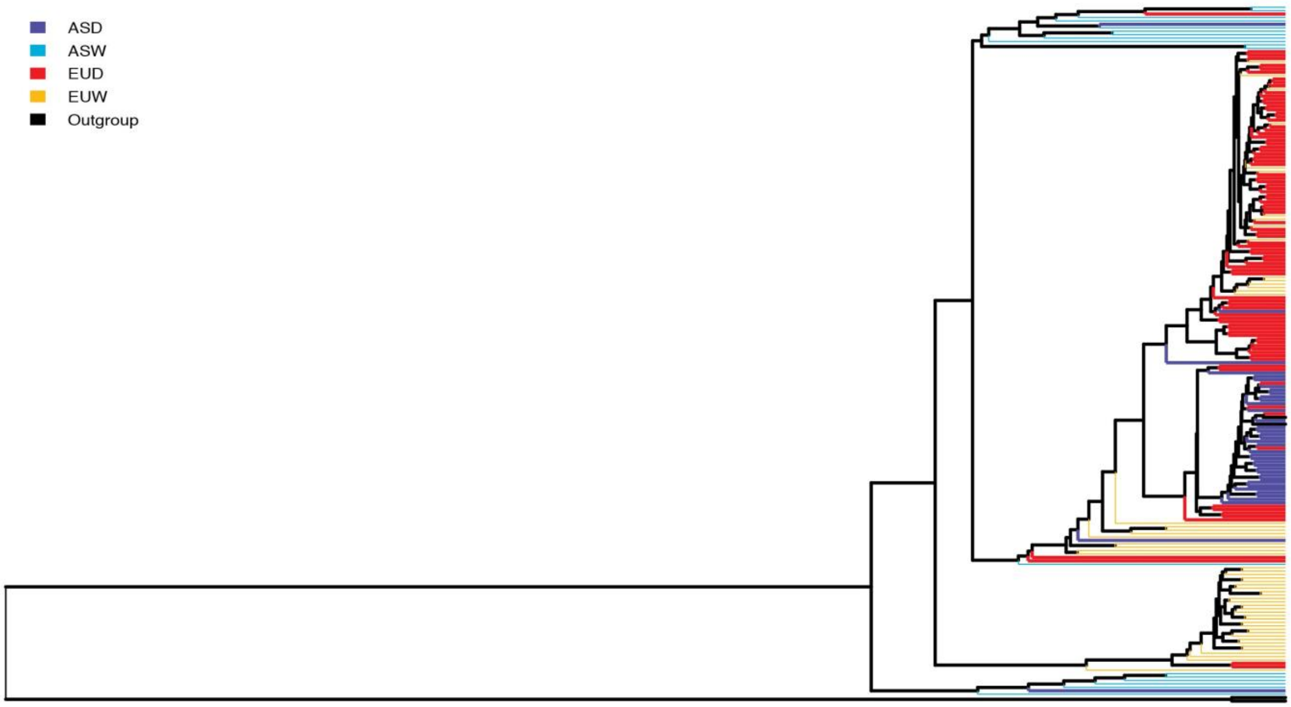

Supplementary Figure 8

Example of genealogy at a sweep region that could be explained by admixture ASD ↔ EUD.

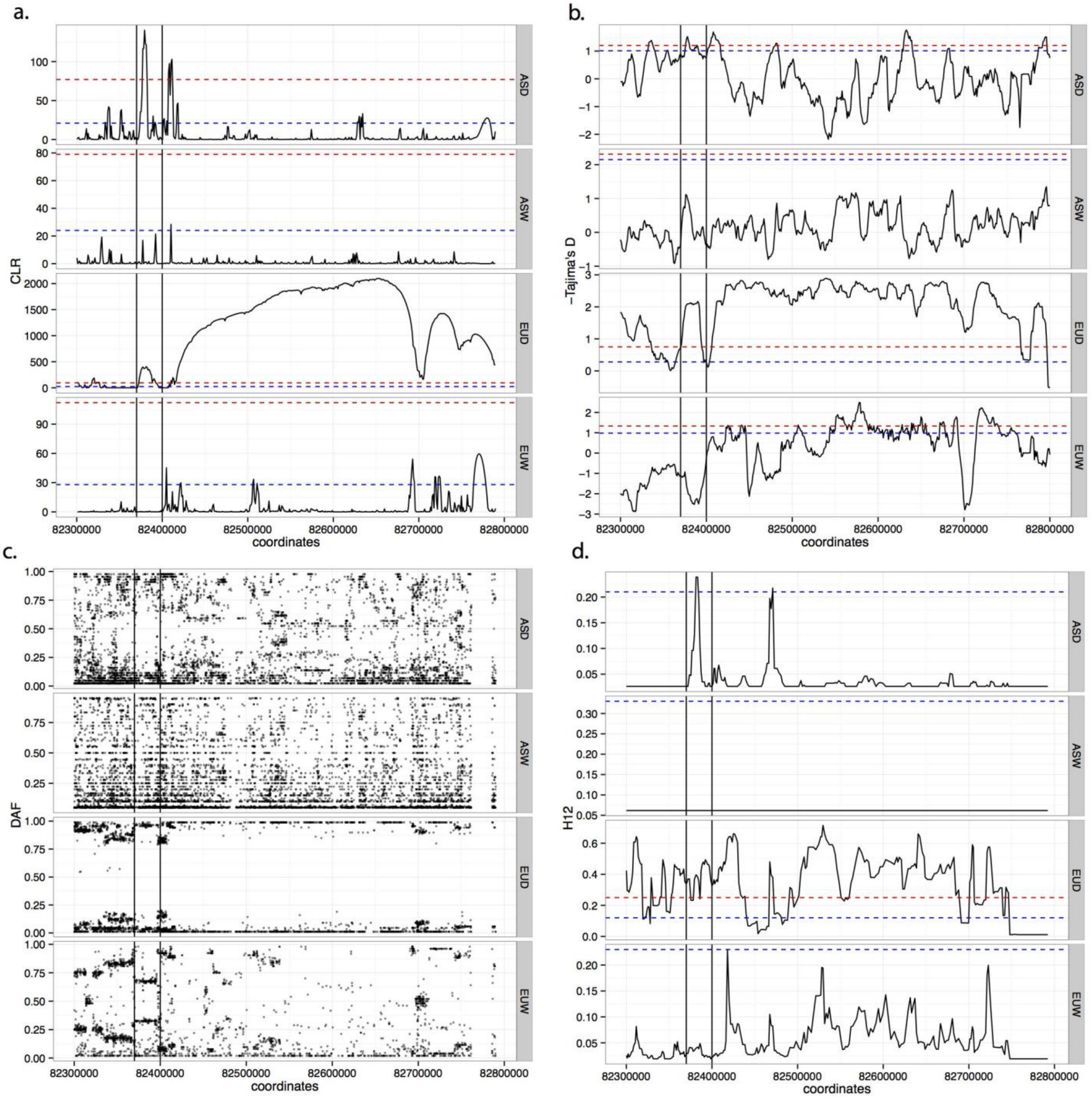

Supplementary Figure 9

Diverse sweep statistics computed in the *PLAG1* region.

Dashed blue and red lines represent thresholds of $P = 0.05$ and $P = 0.01$, respectively. (**a**) CLR. (**b**) DAF. (**c**) Tajima's *D.* (**d**) H12 statistic.

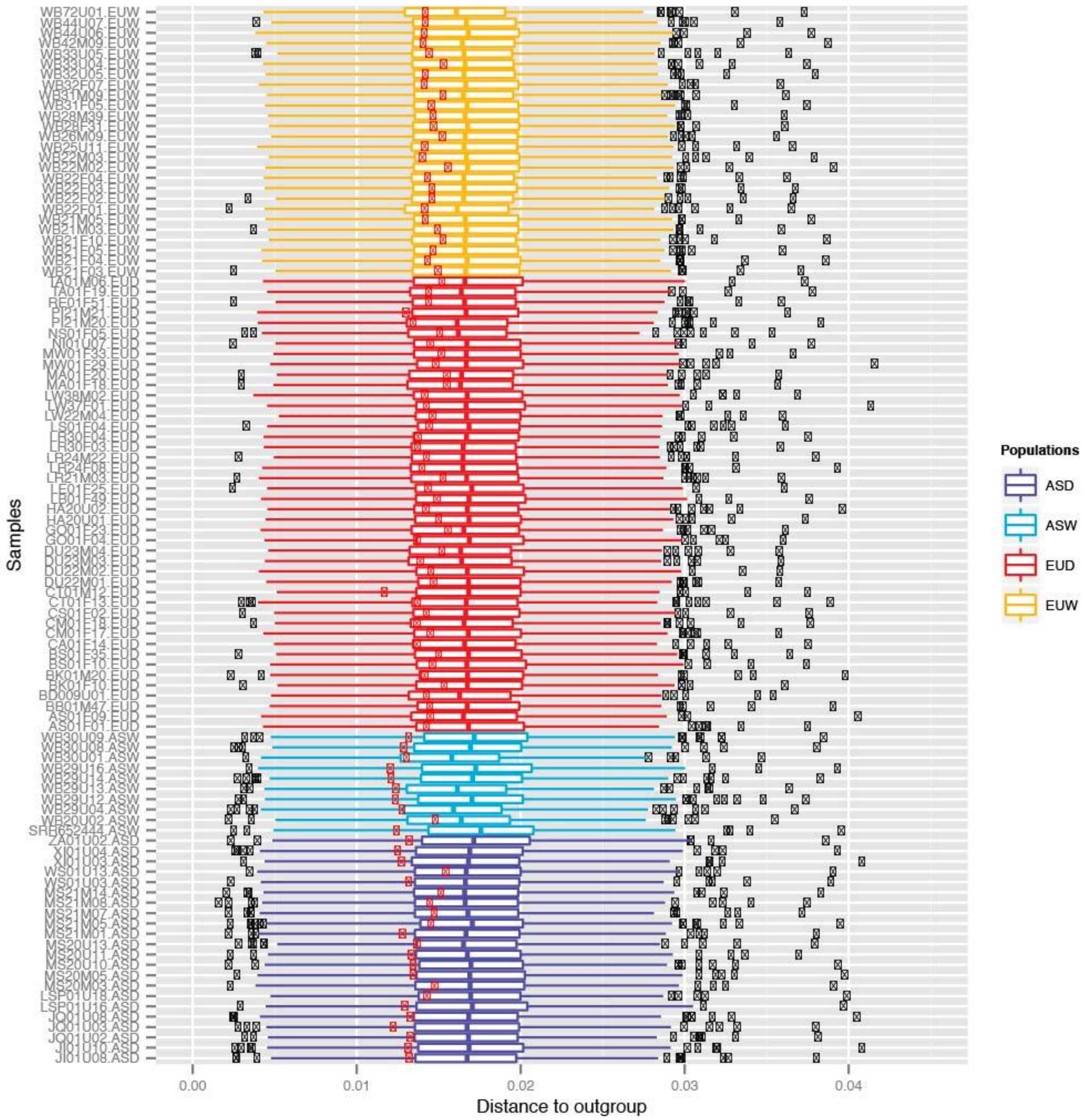

Supplementary Figure 10

Nucleotide divergence relative to the outgroup in the swept region.

Each box plot, for the samples shown along the *y* axis represents the distribution of raw nucleotide divergence relative to the outgroup in 1,000 randomly selected 10-kb bins across the genome. Red dots represent the mean nucleotide divergence relative to the outgroup in the sweep region in **Figure 4**.

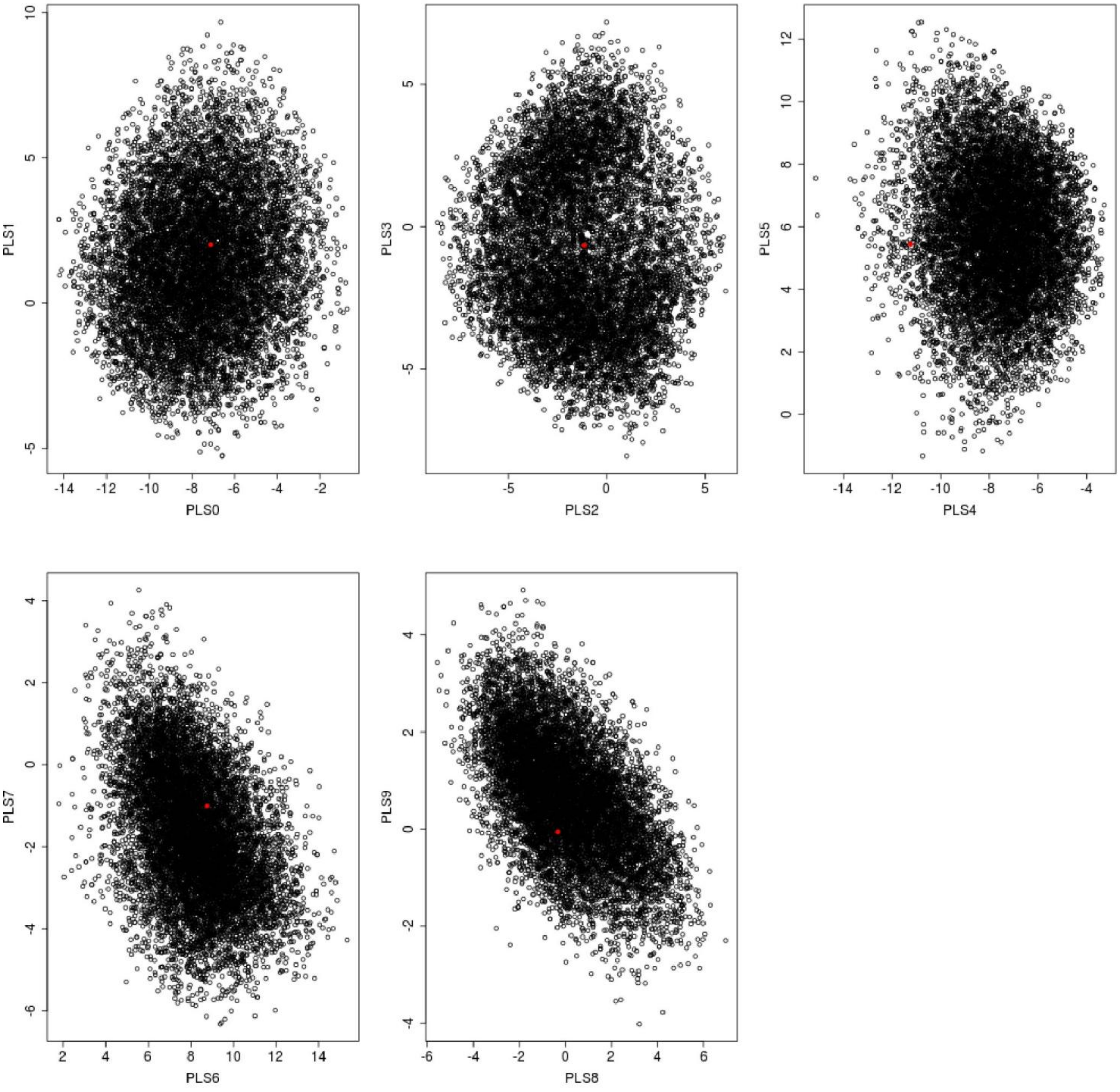

Supplementary Figure 11

PLS distribution of 10,000 (out of 2,000,000) retained simulations and observed data under the full model.

Simulations are shown in black, and observed data are shown in red.

Supplementary Tables

Supplementary Table 1: List of samples used in this study.

See "SuppTable1.xls".

Supplementary Table 2: Support for each model in Supplementary Figure 2.

See "SuppTable2.doc".

Supplementary Table 3: Prior and posterior distributions for the Full model. All population size (N_) and migration rate (m_) parameters are in log scale. All other models (Supplementary Fig. 2) use the same prior bound. RMSE is the root mean square error. P_value_KS corresponds to the p-value of the Kolomogorov-Smirnov of uniformity of the posterior quantiles (see "Validation of ABC procedure").

See "SuppTable3.xls".

Supplementary Table 4: Number of overlapping and unique 10kb sweep regions with p<0.01 in each population.

	EUD	ASD	EUW	ASW
EUD	1953	2	44	0
ASD	2	1014	0	4
EUW	44	0	588	0
ASW	0	4	0	349

Supplementary Table 5: GO terms enriched in EUD.

Gene ontology term	Gene count	P(FDR)
developmental process	26#3347	<0.0001
cellular component organization and biogenesis	24#3277	0.0008
anatomical structure development	17#2005	0.0013
multicellular organismal development	18#2299	0.0027
urogenital system development	3#40	0.0224
cellular developmental process	14#1810	0.0224
cell differentiation	14#1810	0.0224
multicellular organismal process	23#3822	0.0245
cell communication	30#5560	0.0245
vesicle-mediated transport	8#606	0.0252
signal transduction	28#5142	0.0292
multicellular organismal development#system development	13#1605	0.0394
positive regulation of cell adhesion	2#15	0.0394
anatomical structure morphogenesis	10#1047	0.0424
positive regulation of biological process	10#1062	0.0424
nervous system development	8#716	0.0424
blood circulation	4#160	0.0424
circulatory system process	4#160	0.0424
biological regulation	33#6731	0.0440
neuropeptide signaling pathway	4#168	0.0456
mesenchymal cell development	2#24	0.0575
cell development	10#1242	0.0585

Supplementary Table 6: GO terms enriched in ASD.

Gene ontology term	Gene count	P(FDR)
cellular component organization and biogenesis	18#3277	0.0002
establishment of protein localization	8#922	0.0309
protein localization	8#961	0.0309
protein complex assembly	5#340	0.0309
nucleotide metabolic process	5#340	0.0309
macromolecule localization	8#1012	0.0309
nucleobase, nucleoside and nucleotide metabolic process	5#367	0.0313
cellular localization	8#1126	0.0392
protein transport	7#866	0.0392
Odontogenesis	2#25	0.0392
positive regulation of transcription	4#279	0.0455
base-excision repair, AP site formation	1#1	0.0455
optic placode formation involved in camera-type eye	1#1	0.0455
optic placode formation	1#1	0.0455
calcium-independent cell-matrix adhesion	1#1	0.0455
DNA catabolic process	2#35	0.0455
positive regulation of nucleobase and nucleic acid metabolic process	4#289	0.0455
macromolecular complex assembly	6#756	0.0550
anatomical structure morphogenesis	7#1047	0.0591
cellular component assembly	6#813	0.0607
establishment of cellular localization	7#1098	0.0607
regulation of nitrogen compound metabolic process	1#2	0.0607
heme oxidation	1#2	0.0607
nitrogen utilization	1#2	0.0607
regulation of nitrogen utilization	1#2	0.0607
organ morphogenesis	4#362	0.0632

Supplementary Table 7: List of genes with GO term enrichment (p<0.01) in sweep regions in EUD.

See “SuppTable7.xls”.

Supplementary Table 8: List of genes with GO term enrichment (p<0.01) in sweep regions in ASD.

See “SuppTable8.xls”.

Supplementary Note

Quality of re-sequencing data

We assessed the presence of outliers in our data that could influence our ABC analysis (see below). To investigate this issue we computed, for each sample, the average nucleotide distance to the outgroup (Supplementary Fig. 1). We computed the number of fixed derived sites (homozygous derived) and segregating derived sites (heterozygous derived) divided by the total number of sites in the genome, avoiding CpG islands (Tortereau et al. 2012) and repetitive elements in 10kb windows. We then computed the mean distance (across all 10kb windows) in each individual and the mean and standard deviation across all individuals. The results of this analysis are presented in Supplementary Fig. 1. This figure demonstrates the absence of strong outliers in EUD, EUW and ASD. However, some samples in the ASW group have a mean divergence lower or higher than other samples (Supplementary Fig. 1). This is most likely the result of different degree of heterozygosity (Bosse et al. 2012) and/or admixture with the outgroup (Frantz et al. 2013; Ai et al. 2015). Thus, this analysis shows that while all other populations included in the analysis are homogeneous, the ASW are not. This is not surprising given the ancestry of these populations and the possible admixture from ancient species (Frantz et al. 2013; Ai et al. 2015; Frantz et al. 2014). We also performed a Principal Component Analysis (PCA) as implemented in *flashpca* (Abraham & Inouye 2014) using 500,000 randomly selected SNPs (with a 100kb minimum distance between SNPs). The SNPs were ascertained in all populations (Fig. 2a). We also repeated this analysis but with 500,00 SNPs ascertained in ASD+ASW (Fig. 2c) and EUD+EUW (Fig. 2d). This analysis further supports the heterogeneity of ASW (Fig 2c.) but does not support the existence of strong outliers in our data set.

Populations for ABC analysis

To test for reproductive isolation between wild and domestic pigs since domestication, we assess the posterior probability of various models using Approximate Bayesian Computation (ABC; see below). For the ABC analysis we pooled multiple individuals from different ancestry (see below) into four populations: European domestics (EUD), European wild (EUW), Asian domestics (ASD) and Asian wild (ASW). Our PCA analysis (Fig. 2) shows that there here is some genetic differentiation between wild and domestic populations (Fig. 2). To further test this we ran an ADMIXTURE analysis (Alexander et al. 2009), to estimate the optimum number of clusters (K) in our data set. The analysis was performed on the same 500,000 randomly chosen SNPs as for the PCA (see above). We used a 5-fold cross-validation procedure to test the fit K=1 to K=10 clusters to the data. We found K=4 minimize the cross-validation error, and hence to be the optimum number of clusters (Fig. 3). The result of this analysis shows that wild populations were all well defined, while domestic populations shared significant amounts of ancestry with wild populations (Fig. 3). The domestic individual with the most shared ancestry with EUW are from the non-commercial breeds Mangalica, Cassertana, Chato Murciano, Retinto and Negro Iberico (Fig. 3; Supplementary Table 1).

ABC

102 genomes were used for the ABC analysis. Simulations were performed on 100 10kbp unlinked loci. To match these simulations we filtered out 10kb loci with more than 10% missing data (from the variant calling step) in all 104 genomes. We also filtered out any loci containing CpG islands and within 100kb of coding sequences. We then required that all loci were separated by at least 100kb to limit the effect of linkage. We polarized mutations using the genome of a Java Warty pig (*S. verrucosus*) (Frantz et al. 2013). Lastly we randomly selected 100 loci that met these criteria. Backward coalescent simulations with recombination were performed using *ms* (Hudson 2002) under 7 models (Supplementary Fig. 2). Supplementary Table 3 recapitulates the priors used for the model parameters. For model testing purposes, we ran 200,000 simulations per model. For each simulation we computed summary statistics, solely based on allele frequency to avoid phasing issues, using libsequence (Thornton 2003). For each population, we computed the number of segregating sites (S), number of private mutations (n1), nucleotide diversity (pi), ThetaW, ThetaH, Tajima’s D, and Fay and Wu’s H. In addition, we computed Fst as well as all other statistics for each pair of populations. For model testing we choose a set of informative summary statistics with a Partial Least Squares Discriminant Analysis as in (Peter et al. 2012) using the '*plsda*' function in R (Lê Cao et al. 2009). We compared all models simultaneously using a standard ABC-GLM approach as implemented in *ABCtoolbox* (Wegmann et al. 2010).

For parameters inference we ran 2,000,000 simulations under the full migration model (Fig 1a; Supplementary Fig. 2). We did not use the ghost model for parameter inference because of the higher number of parameters in this model (6 extra: 1 Ne, 1 time, 4 migrations) that increases parameter space. Moreover, given we have no data about this ghost population, these parameters cannot be accurately estimated with the current approach (Hammer et al. 2011). We extracted 10 Partial Least Square (PLS) components from the 93 summary statistics in the observed and simulated data (Wegmann et al. 2009; Supplementary Fig. 11). We retained a total of 10,000 simulations closest to the observed data and applied a standard ABC-GLM (Leuenberger & Wegmann 2010). We checked for bias in the prior using 1,000 pseudo observed data (POD) sets with known parameters value (Wegmann & Excoffier 2010). We then computed the coverage properties of the posterior distribution using our 10,000 closets simulations. Uniformity was assessed using a classical Kolmogorov-Smirnov test for each parameter independently (Wegmann & Excoffier 2010) (Supplementary Table 3). We evaluated the power of our approach to infer each parameter using the 1,000 POD by computing root mean square error of the mode (RMSEmode; Supplementary Table 3) for known parameters (Wegmann & Excoffier 2010). In order to check if the data is in agreement with the assumed model we computed the distribution of the marginal densities of the 10,000 retained simulations for posterior estimation and computed the fraction of simulation with smaller marginal densities than the observed data set (Wegmann & Excoffier 2010).

Validation of ABC procedure

To validate our model testing procedure, we used 1,000 pseudo-observed datasets (POD). We found that our approach can recover the right model for 899 out of 1,000 POD. In addition, we found that under all models but model 4, the full model and the ghost model (Supplementary Fig. 2), all retained simulation had higher marginal likelihood than the observed data for all models. This suggests that these models provided a very poor fit to this genomic dataset. In contrast, we found that the fraction of simulation with lower marginal likelihood was 0.009 for model 4, 0.043 for the full model and 0.1 for the ghost model. This suggests that these models are capable of reproducing the observed summary statistics (10 PLS components; Supplementary Table 3) (Peter et al. 2012; Wegmann & Excoffier 2010). We also used 1,000 POD under the full model to check for biased prior during parameter estimation. To do so, we checked the uniformity of the posterior quantile distribution using a Kolomogorov-Smirnov test for each parameter (see above) as suggested by (Wegmann et al. 2009). We found that most parameter had a uniform distribution (Supplementary Table 3). Lastly, we also checked if the raw summary statistics were consistent with the simulations. To do so, we plotted the distribution of multiple summary statistics obtained from the 10,000 closest simulations retained from the model testing procedure under the null and full model (Supplementary Fig. 2). All observed summary statistics fell within the distribution of the simulated data (Supplementary Fig. 3). In addition, in most case the observed summary statistics were closer to the summary statistics simulated under the full model than the null model (Supplementary Fig. 3). Some of the summary statistics were more informative than others (i.e. Fst is more informative S [number of segregating sites] or n1 [number of singletons]; Supplementary Fig. 3).

Ancestry of wild and domestic pigs

To further support our claim of gene-flow between wild and domestic pigs, we assessed the ancestry of our populations using 622 pigs from the same populations as above, that were genotyped using the Porcine SNP60 array (Supplementary Table 1; (Ramos et al. 2009)). We first performed a Principal Component Analysis (PCA) as implemented in *flashpca* (Abraham & Inouye 2014) to investigate the relationship among these populations. Unsurprisingly, we found that the first PC discriminates between Asian and European pigs (Supplementary Fig. 6). This is in line with previous studies that found that European and Asian wild boar populations likely diverged around 1My ago (Frantz et al. 2013; Groenen et al. 2012). In addition, we found that none of the PCs discriminate among Asian populations (Supplementary Fig. 6&7), while PC3-4 show clear differentiation among most European breeds (Supplementary Fig. 7). This result is most likely due to the fact that the Porcine SNP60 chip was ascertained in European commercial pigs (Ramos et al. 2009). We repeated this analysis based on SNPs from our 103 genomes (see above). This analysis further demonstrates the ascertainment bias of the Porcine SNP60 chip in EUD. Indeed, Fig. 2a shows the exact opposite pattern, with Asian pigs being more variable, consistent with the hypothesis that this species originated in East Asia (Groenen et al. 2012; Frantz et al. 2013). To further investigate historical relationship among these populations we used *TreeMix* (Pickrell & Pritchard 2012) to fit a bifurcating tree to our 60K dataset. Surprisingly, we found that EUD and ASD are paraphyletic, while EUW are monophyletic (Supplementary Fig. 4). To validate this finding we build a neighbor joining phylogeny (using the BIONJ function in the “ape” R package (Paradis et al. 2004)) of our 103 genomes based IBS distance matrix as computed by plink (Purcell et al. 2007) using the same set of 500,000 random

SNPs as for the PCA (see above). This analysis confirms the paraphyly of both ASD and EUD (Fig. 2b). Such a finding is difficult to reconcile with a simple model of domestication that involves a single source population and/or little gene-flow between wild and domestics. However, paraphyly and complex ancestry in domestic pigs could be the result of multiple events of interbreeding with wild-boars as well as interbreeding between Asian and European domestics during the 19th century industrial revolution (White 2011a; Groenen et al. 2012; Bosse et al. 2014). Nevertheless, our samples include many non-commercial breeds that are unlikely to be heavily admixed with Asian domestics (White 2011; Porter 1993).

Migration rates

To further test the hypothesis that gene-flow between ASD and EUD did not influence our findings we simulated 2 million samples under the best fitting model and used ABC to estimate the posterior distribution of migration rates (see above). We found that rate of gene flow EUW → EUD was quite high. We estimate $m_{EUW,EUD}$ (fraction of the EUD population made up of EUW migrants each generation) to be $1.1x10^{-4}$ (mode; 95% HPDI [$1.3x10^{-6}$-$1.7x10^{-3}$]; Supplementary Table 3), corresponding roughly to 2.3 migrants/generations. On the other hand we found that the rate of gene-flow EUD → EUW was quite low with $m_{EUD,EUW}$=$5.6x10^{-6}$ (mode; 95% HPDI [$8.9x10^{-7}$-$9.1x10^{-4}$]; Supplementary Table 3), corresponding roughly to 0.05 migrants/generation. This pattern was slightly reversed in Asia with $m_{ASD,ASW}$=$1.5x10^{-4}$ (mode; 95% HPDI [$2.4x10^{-6}$-$2.3x10^{-3}$]; Supplementary Table 3; ~5.6 migrants/generations) and $m_{ASW,ASD}$=$8.9x10^{-5}$ (mode; 95% HPDI [$2.4x10^{-6}$-$2.2x10^{-3}$]; Supplementary Table 3; ~2.3 migrants/generations). However, the pattern in Asia is difficult to interpret due to the large confidence interval (HPDI; Supplementary Table 3) most likely due to the complex history of ASW as well as the limited number of sequences in ASW. Lastly, the rate of migration between the two domestic populations (ASD and EUD) was much lower, with $m_{EUD,ASD}$ =$6.5x10^{-6}$ (mode; 95% HPDI [8.9^{-7}-$1.1x10^{-3}$]; Supplementary Table 3; ~ 0.17 migrants/generation) and $m_{ASD,EUD}$=$7.1x10^{-6}$ (mode; 95% HPDI [$8.8x10^{-7}$-$7.1x10^{-4}$]; Supplementary Table 3; ~0.14 migrants/generation). This result suggests that the gene-flow between ASD and EUD did not confound our findings that gene-flow took place between wild and domestic pigs.

Demography of Asian pigs

The same possible population decline as highlighted in the main text was observed in ASW and ASD (Supplementary Fig. 5; Fig. 4). This is also consistent with Pleistocene glaciation-induced population decline (Frantz et al. 2013; Groenen et al. 2012; Bosse et al. 2014). Nevertheless, we found that contrary to European pigs, ASW had a higher effective population size (Ne_{ASW}=35,933; 95% HPDI [6,313-97,702]) than ASD (Ne_{ASD}=25,947; 95% HPDI [4,906-97,002]). The proportions of retained simulations were Ne_{ASW} was greater than Ne_{ASD} was 0.56 (5,602 out of 10,000). However, for modelling purposes, as well as due to the limited number of wild boars from Asia available in the study, we made the assumption that all Asian wild boars form a single population. Indeed, given the common history of ASD and EUD (White 2011a; Groenen et al. 2012; Bosse et al. 2014) it was necessary for our models to be realistic to include a surrogate population for ASW. Nevertheless, this assumption likely influenced our demographic analysis in China; as it was shown previously that population from North and South China show much greater genetic differentiation than between any modern European wild boar populations (Larson et al. 2005; Frantz et al. 2013; Groenen et al. 2012; Bosse et al. 2012). In addition, North and South Chinese wild boars did not form a monophyletic clade in our 60K SNP analysis (Supplementary Fig. 4). Such unaccounted-for long-term substructure likely influenced, our quality report (Supplementary Fig. 1). Moreover, possible ancient admixture (Frantz et al. 2013; Frantz et al. 2014; Ai et al. 2015) makes it difficult to draw strong conclusions about demography of domestication in Chinese pigs. However, this finding is not expected to have any influence on the conclusion from our gene-flow analysis. Indeed, substructure within ASD could result in artificial migration ASD → ASW, if one of the ASW subpopulation was closer to ASD, but substructure cannot explain the migration ASW → ASD if ASD were genetically isolated.

Time of domestication

Our models also include time parameters that represent the time of domestication (T_1 and T_2 in Supplementary Fig. 2). However, our ABC validation step suggests that our current approach/data is expected to provide little power to retrieve these parameters. Indeed, the RMSE for T_1 and T_2 was around 2.5 (Supplementary Table 3). This lack of power is reflected in the shape of our posterior distribution for these parameters (Supplementary Table 3). While the uniformity of these posterior distributions could be an artefact of our choice of summary statistics, it is more likely due to the fact that there is no strong signal for a sharp domestication episode. This supports our view that domestication of is a diffuse, long-term process, and may indicate that it is ultimately futile to try to infer the precise timing of the onset of domestication in pigs.

Selection scan

We used *SweeD* to detect sweeps (Pavlidis et al. 2013). The program was run for each population separately using all available SNPs. The highest composite likelihood ratio (CLR) score for every 10kb interval was used for further analysis. To obtain critical threshold values (p-values), we used a posterior predictive simulation (PPS) approach. We simulated 2 replicates of 3Mbp each using the parameters of the 10,000 closest retained simulations from our ABC analysis (20,000 simulations). Simulations were run using macs (Chen et al. 2009). We derived a critical threshold for observed CLR in each population using the cumulative descriptive function (CDF) derived from the CLR distribution that was obtained from the PPS. All regions with p<0.01 were selected for further analysis. Supplementary Table 5 and 6 provide a list of terms enriched in EUD and ASD respectively. We computed the overlap of these regions between populations and defined set of regions unique to each population as well as overlapping only between ASD and EUD (Supplementary Table 4). These sweep coordinates were then overlapped with the Ensembl (v75) gene annotation. We tested for enrichment of gene ontology term in each population using a fisher-exact test with a Benjamini-Hochberg correction for multiple testing as implemented in the Gostat program (Beissbarth & Speed 2004). We only considered genes with human orthology (Goa-human).

To perform phylogenetic analysis, we first extracted 20kb bp around putative parallel sweeps. We then phased these regions in BEAGLE 4 (Browning & Browning 2007) using default settings. We then built trees using UPGMA as implemented in the R package Phangorn (Schliep 2011) after computing Kimura-2-parameter model corrected distances using the R package ape (Paradis et al. 2004).

To validate the sweep in Figure 5 we computed the derived allele frequency (DAF), Tajima's D and a haplotype based method (H12; Garud et al. 2015). The results are presented in

Supplementary Fig. 9. Each of these methods provides a clear-cut signal for a sweep in EUD as shown in Fig. 5 (PLAG1 region). Moreover, Supplementary Fig. 9 shows that the signal in the upstream region (Fig. 5b) is also significant in and only in ASD and EUD under various methods. We also investigated whether the signal in this sweep region could be the result of an elevated mutation rate in this region. To do so, we computed nucleotide divergence to the outgroup (see section "Quality of re-sequencing data") in 1,000 randomly selected 10kb windows across the genome, as well as the sweep region in Fig. 5, for every individual. The results of this analysis are presented in Supplementary Fig. 10. We found that the nucleotide divergence to the outgroup was slightly lower in this region than in the rest of the genome; thus ruling out any effect of accelerated mutation rate influencing our sweep analysis in this region.

Genes under positive selection in domestic pigs

We ensured that each sweeps in domestic populations was not overlapping with a sweep in a wild population (see main text). Supplementary Table 5 and 6 provide a list of term enriched in EUD and ASD respectively and Supplementary Table 7 and 8 provide a full list of the genes overlapping with sweeps. These terms comprise multiple gene candidates related to height (*PLAG1*, *NCPAG*, *PENK*, *RPS20* and *LYN* in EUD; *LEMD3* and *UPK1* in ASD) in pigs (Andersson-Eklund et al. 1998; Rubin et al. 2012) and cattle (Karim et al. 2011; Saatchi et al. 2014) as well as candidates that affect bone and teeth formation (*GERM1*, *PLCL1* in EUD; *PKD1*, *LEMD3*, *SCL4A4*, *ENAM* and *AMTN* in ASD) (Canalis et al. 2012; Nagatomo et al. 2008; Gazzerro et al. 2007; Aggarwal 2013; Hellemans et al. 2004; Jalali et al. 2014; Lacruz et al. 2010; Hu et al. 2014; Coxon et al. 2012; Dos Santos Neves et al. 2012). We also found genes involved in development of hippocampal neurons (*NRTN*) (Quartu et al. 2005; Simanainen et al. 2013), axon guidance (*SEMA3C* and *PLXNC1*) (Oschipok et al. 2008; Hernández-Montiel et al. 2008; Gonthier et al. 2007; Ruediger et al. 2013; Niquille et al. 2009; Pasterkamp et al. 2007), neural crest development (*SEMA3C* and *NRTM*) (Brown et al. 2001) and dentrite growth regulation (*AAK1*) (Ultanir et al. 2012). In addition, we found candidate genes in ASD involved in neurite growth (*RAB35*) (Chevallier et al. 2009) and central nervous system development (*GGA2* and *FRS2*) (Borgonovo et al. 2012; López-Aranda et al. 2008; Ong et al. 2000). Finally, we identified genes that have been shown to directly affect or regulate behavioural traits (*i.e.* aggressiveness and feeding behaviour) in EUD (*APBA2*, *MC4R*, *RCAN1*) (Sokol et al. 2006;

Grayton et al. 2013; Bhoiwala et al. 2013; Dierssen et al. 2011; Kim et al. 2000; Xu et al. 2013; Valette et al. 2013) and in ASD (*BAIPA3*) (Wojcik et al. 2013).

Purifying selection.

In order to investigate the effect of purifying selection on the genome of domestic and wild pigs we used the *PhyloP* (Pollard et al. 2009) annotation provided by UCSC. *PhyloP* scores are a base-wise statistics that measure acceleration or conservation based on a multi-species alignment. Low scores (below 0) imply accelerated evolution, while high scores (greater than 0) imply conservation. Here we used the *PhyloP* 60-way vertebrate, obtained for the mouse genome (mm10) from UCSC. We used *liftOver* (Hinrichs et al. 2006) and the chain file mm10ToSusScr3.over.chain provided by UCSC to lift the coordinate from mm10 to susScr3. Thereafter, we randomly selected 500,000 SNPs from our set of 102 pig samples, for which we computed derived allele frequency (DAF) and F_{st} between wild and domestic (F_{st} ASD-ASW and EUD-EUW). We then used R to compute a correlation coefficient (Pearson's product-moment) between DAF / F_{st} and *PhyloP* scores. We found that the DAF was negatively correlated with *PhyloP* scores in all populations (ASD: ρ=-0.061, p<2.2e-16; ASW: ρ=-0.062, p<2.2e-16; EUD: ρ=-0.063, p<2.2e-16; EUW: ρ=-0.062, p<2.2e-16). We also found a negative correlation between F_{st} and *PhyloP* score (F_{st} EUD-EUW: ρ=-0.009, p=2.2e-10; F_{st} ASD-ASW: ρ=-0.008, p=9.3e-10). Together these results suggest that high frequency derived alleles are less conserved than expected by chance and that highly conserved sites are less affected by artificial selection (as shown by the lower Fst).

References

Abraham, G. & Inouye, M., 2014. Fast principal component analysis of large-scale genome-wide data. Y. Zhang, ed. PloS one, 9(4), p.e93766.

Aggarwal, S., 2013. Skeletal dysplasias with increased bone density: evolution of molecular pathogenesis in the last century. Gene, 528(1), pp.41–5.

Ai, H. et al., 2015. Adaptation and possible ancient interspecies introgression in pigs identified by whole-genome sequencing. Nature Genetics, in press.

Alexander D.H., Novembre J., and Lange K., 2009. Fast model-based estimation of ancestry in unrelated individuals. Genome Research, 19, pp.1655–1664.

Andersson-Eklund, L. et al., 1998. Mapping quantitative trait loci for carcass and meat quality traits in a wild boar x Large White intercross. Journal of animal science, 76(3), pp.694–700.

Beissbarth, T. & Speed, T.P., 2004. GOstat: find statistically overrepresented Gene Ontologies within a group of genes. Bioinformatics, 20(9), pp.1464–5.

Bhoiwala, D.L. et al., 2013. Overexpression of RCAN1 isoform 4 in mouse neurons leads to a moderate behavioral impairment. Neurological research, 35(1), pp.79–89.

Borgonovo, J. et al., 2012. Expression of coat proteins changes during postnatal development in selected areas of the rat brain. International journal of developmental neuroscience : the official journal of the International Society for Developmental Neuroscience, 30(4), pp.333–41.

Bosse, M., Megens, H.-J., Frantz, L.A.F., Madsen, O., Larson, G., Paudel, Y., Duijvesteijn, N., Harlizius, B., Hagemeijer, Y., Crooijmans, R.P.M.A. & Groenen, M.A.M., 2014. Genomic analysis reveals selection for Asian genes in European pigs following human-mediated introgression. Nature communications, 5, p.4392.

Bosse, M. et al., 2012. Regions of homozygosity in the porcine genome: consequence of demography and the recombination landscape. PLoS genetics, 8(11), p.e1003100.

Bosse, M., Megens, H.-J., Madsen, O., et al., 2014. Untangling the hybrid nature of modern pig genomes: a mosaic derived from biogeographically distinct and highly divergent Sus scrofa populations. Molecular ecology.

Brown, C.B. et al., 2001. PlexinA2 and semaphorin signaling during cardiac neural crest development. Development, 128(16), pp.3071–3080.

Browning, S.R. & Browning, B.L., 2007. Rapid and accurate haplotype phasing and missing-data inference for whole-genome association studies by use of localized haplotype clustering. American journal of human genetics, 81(5), pp.1084–97.

Canalis, E., Parker, K. & Zanotti, S., 2012. Gremlin1 is required for skeletal development and postnatal skeletal homeostasis. Journal of cellular physiology, 227(1), pp.269–77.

Chen, G.K., Marjoram, P. & Wall, J.D., 2009. Fast and flexible simulation of DNA sequence data. Genome research, 19(1), pp.136–42.

Chevallier, J. et al., 2009. Rab35 regulates neurite outgrowth and cell shape. FEBS letters, 583(7), pp.1096–101.

Coxon, T.L. et al., 2012. Phenotype-genotype correlations in mouse models of amelogenesis imperfecta caused by Amelx and Enam mutations. Cells, tissues, organs, 196(5), pp.420–30.

Dierssen, M. et al., 2011. Behavioral characterization of a mouse model overexpressing DSCR1/ RCAN1. PloS one, 6(2), p.e17010.

Frantz, L.A. et al., 2013. Genome sequencing reveals fine scale diversification and reticulation history during speciation in Sus. Genome biology, 14(9), p.R107.

Frantz, L.A.F. et al., 2014. Testing models of speciation from genome sequences: divergence and asymmetric admixture in Island Southeast Asian Sus species during the Plio-Pleistocene climatic fluctuations. Molecular ecology in press.

Garud, N.R. et al., 2015. Recent Selective Sweeps in North American Drosophila melanogaster Show Signatures of Soft Sweeps. PLoS genetics, 11(2), p.e1005004.

Gazzerro, E. et al., 2007. Conditional deletion of gremlin causes a transient increase in bone formation and bone mass. The Journal of biological chemistry, 282(43), pp.31549–57.

Gonthier, B. et al., 2007. Functional interaction between matrix metalloproteinase-3 and semaphorin-3C during cortical axonal growth and guidance. Cerebral cortex, 17(7), pp.1712–21.

Grayton, H.M. et al., 2013. Altered social behaviours in neurexin 1α knockout mice resemble core symptoms in neurodevelopmental disorders. V. Trezza, ed. PloS one, 8(6), p.e67114.

Groenen, M.A.M. et al., 2012. Analyses of pig genomes provide insight into porcine demography and evolution. Nature, 491(7424), pp.393–398.

Hammer, M.F. et al., 2011. Genetic evidence for archaic admixture in Africa. Proceedings of the National Academy of Sciences of the United States of America, 108(37), pp.15123–8.

Hellemans, J. et al., 2004. Loss-of-function mutations in LEMD3 result in osteopoikilosis, Buschke-Ollendorff syndrome and melorheostosis. Nature genetics, 36(11), pp.1213–8.

Hernández-Montiel, H.L. et al., 2008. Semaphorins 3A, 3C, and 3F in mesencephalic dopaminergic axon pathfinding. The Journal of comparative neurology, 506(3), pp.387–97.

Hinrichs AS, et al., 2006. The UCSC Genome Browser Database: update 2006. Nucleic Acids Res. 34, pp. D590-8

Hu, J.C.-C. et al., 2014. Enamelin is critical for ameloblast integrity and enamel ultrastructure formation. PloS one, 9(3), p.e89303.

Hudson, R.R., 2002. Generating samples under a Wright-Fisher neutral model of genetic variation. Bioinformatics, 18(2), pp.337–338.

Jalali, R. et al., 2014. NBCe1 (SLC4A4) a potential pH regulator in enamel organ cells during enamel development in the mouse. Cell and tissue research.

Karim, L. et al., 2011. Variants modulating the expression of a chromosome domain encompassing PLAG1 influence bovine stature. Nature genetics, 43(5), pp.405–13.

Kim, K.S. et al., 2000. A missense variant of the porcine melanocortin-4 receptor (MC4R) gene is associated with fatness, growth, and feed intake traits. Mammalian Genome, 11(2), pp.131–135.

Lacruz, R.S. et al., 2010. The sodium bicarbonate cotransporter (NBCe1) is essential for normal development of mouse dentition. The Journal of biological chemistry, 285(32), pp.24432–8.

Larson, G. et al., 2005. Worldwide phylogeography of wild boar reveals multiple centers of pig domestication. Science (New York, N.Y.), 307(5715), pp.1618–21.

Lê Cao, K.-A., González, I. & Déjean, S., 2009. integrOmics: an R package to unravel relationships between two omics datasets. Bioinformatics (Oxford, England), 25(21), pp.2855–6. Leuenberger, C. & Wegmann, D., 2010. Bayesian computation and model selection without likelihoods. Genetics, 184(1), pp.243–52.

López-Aranda, M.F. et al., 2008. A dynamic expression pattern of sGalpha(i2) protein during early period of postnatal rat brain development. International journal of developmental neuroscience : the official journal of the International Society for Developmental Neuroscience, 26(6), pp.611–24.

Nagatomo, K.J. et al., 2008. Transgenic overexpression of gremlin results in developmental defects in enamel and dentin in mice. Connective tissue research, 49(6), pp.391–400.

Niquille, M. et al., 2009. Transient neuronal populations are required to guide callosal axons: a role for semaphorin 3C. PLoS biology, 7(10), p.e1000230.

Ong, S.H. et al., 2000. FRS2 Proteins Recruit Intracellular Signaling Pathways by Binding to Diverse Targets on Fibroblast Growth Factor and Nerve Growth Factor Receptors. Molecular and Cellular Biology, 20(3), pp.979–989.

Pollard K.S., Hubisz M.J., Siepel A., 2006. Detection of non-neutral substitution rates on mammalian phylogenies. Genome Research. 20(1), pp.110-21.